

Weighted compositional functional data analysis for modeling and forecasting life-table death counts

Han Lin Shang  *

Department of Actuarial Studies and Business Analytics
Macquarie University

Steven Haberman 

Bayes Business School
City St George's, University of London

Abstract

Age-specific life-table death counts observed over time are examples of densities. Non-negativity and summability are constraints that sometimes require modifications of standard linear statistical methods. The centered log-ratio transformation presents a mapping from a constrained to a less constrained space. With a time series of densities, forecasts are more relevant to the recent data than the data from the distant past. We introduce a weighted compositional functional data analysis for modeling and forecasting life-table death counts. Our extension assigns higher weights to more recent data and provides a modeling scheme easily adapted for constraints. We illustrate our method using age-specific Swedish life-table death counts from 1751 to 2020. Compared to their unweighted counterparts, the weighted compositional data analytic method improves short-term point and interval forecast accuracies. The improved forecast accuracy could help actuaries improve the pricing of annuities and setting of reserves.

Keywords: age distribution of death counts; geometrically decaying weights; centered log-ratio transformation; weighted principal component analysis

*Corresponding author. Telephone number: +61(2) 9850 4689; Email: hanlin.shang@mq.edu.au

1 Introduction

Actuaries and demographers have long been interested in developing mortality modeling and forecasting methods. In the literature on human mortality, three functions are widely considered: hazard, survival, and probability density functions. Although these functions are complementary (Preston et al. 2001, Dickson et al. 2009), most attention was given to new approaches for forecasting age-specific hazard function (see, e.g., Booth 2006, Booth & Tickle 2008, for reviews). Instead of modeling central mortality rates, we consider modeling the life-table death distribution (see, e.g., Basellini et al. 2020). Observed over a period, we could model and forecast a redistribution of the density of life-table death counts, where deaths at younger ages are shifted gradually toward older ages. The period life-table death counts represent the mortality conditions, which, in recent years, have reflected a trend toward increasing longevity. Apart from providing an informative description of the mortality experience of a population, the life-table death counts yield readily available information on ‘central longevity indicators’ (see, e.g., Cheung et al. 2005, Canudas-Romo 2010), and lifespan variability (see, e.g., Robine 2001, Vaupel et al. 2011, Horiuchi et al. 2013, van Raalte & Caswell 2013, van Raalte et al. 2014, Aburto & van Raalte 2018, Aburto et al. 2020).

In demography, Oeppen (2008) and Bergeron-Boucher et al. (2017, 2018) treat life-table death counts as compositional data and use compositional data analysis (CoDa) to model and forecast age distribution of death counts. The data are constrained to vary between two limits (e.g., 0 and a constant upper bound), which in turn imposes constraints upon the variance-covariance structure of the original data. To remove the non-negativity and most of the summability constraints, the centered log-ratio transformation (Aitchison & Shen 1980, Aitchison 1982, 1986) can be deployed before applying principal component analysis to the transformed data.

In actuarial science, Shang & Haberman (2020) and Shang et al. (2022) apply the centered log-ratio transformation within the CoDa framework to model and forecast life-table death counts. The main contribution of this paper is that we extend the CoDa by assigning a set of geometrically decaying weights to estimate the geometric mean function and the estimated principal component decomposition. As described in Section 3, our extension assigns higher weights to relatively more recent data to improve short-term forecast accuracy. This extension is particularly important in demography, where we can have over 250 years of data, and data from the 18th and 19th centuries may not be so helpful in determining the recent trend for forecasting.

In statistics, Scealy et al. (2017) apply CoDa to study the concentration of chemical elements in sediment or rock samples. Scealy & Welsh (2017) apply CoDa to analyze total weekly expenditure on food and housing costs for households in a chosen set of domains. Stefanucci & Mazzuco (2022) apply CoDa to model cause-specific mortality data. Delicado (2011) and Romano et al. (2021) use CoDa to analyse density functions over space, while Kokoszka et al. (2019) model and forecast a

time series of density functions.

Using Swedish life-table death counts from 1751 to 2020 in Section 2, we highlight the difference between the weighted and standard CoDa methods in Section 3. In Section 4, we study the optimal selection of weight parameters for each horizon by minimizing point and interval forecast errors. We evaluate and compare point forecast accuracy in Section 5 and interval forecast accuracy in Section 6, respectively. The conclusion is presented in Section 7, along with some ideas on how the methodology can be further extended.

2 Swedish age distribution of death counts

We consider age- and sex-specific life-table death counts from 1751 to 2020 in Sweden, the country with the longest record in the [Human Mortality Database \(2024\)](#). For over 250 years, each parish in Sweden has kept a complete and continuously updated register of its population (see [Glei et al. 2007](#)). We study life-table death counts, where the life-table radix (i.e., a population experiencing 100,000 births annually) is fixed at 100,000 at age 0 for each year. For the life-table death counts, there are 111 ages, and these are ages $0, 1, \dots, 109, 110+$. Due to rounding, there are zero counts for age 110+ at some years, which may create an issue when taking log-ratio transformation. To rectify this problem, we use the probability of dying and the life-table radix to recalculate our estimated death counts (up to 6 decimal places). In doing so, we obtain more precise death counts than the ones reported in the [Human Mortality Database \(2024\)](#), which are often reported as integers. To some extent, the probability of dying relies on smooth rates (see the [Human Mortality Database 2024](#), protocol for detail). Figure 1 presents rainbow plots of the female and male age-specific period life-table death counts in Sweden from 1751 to 2020 in single years.

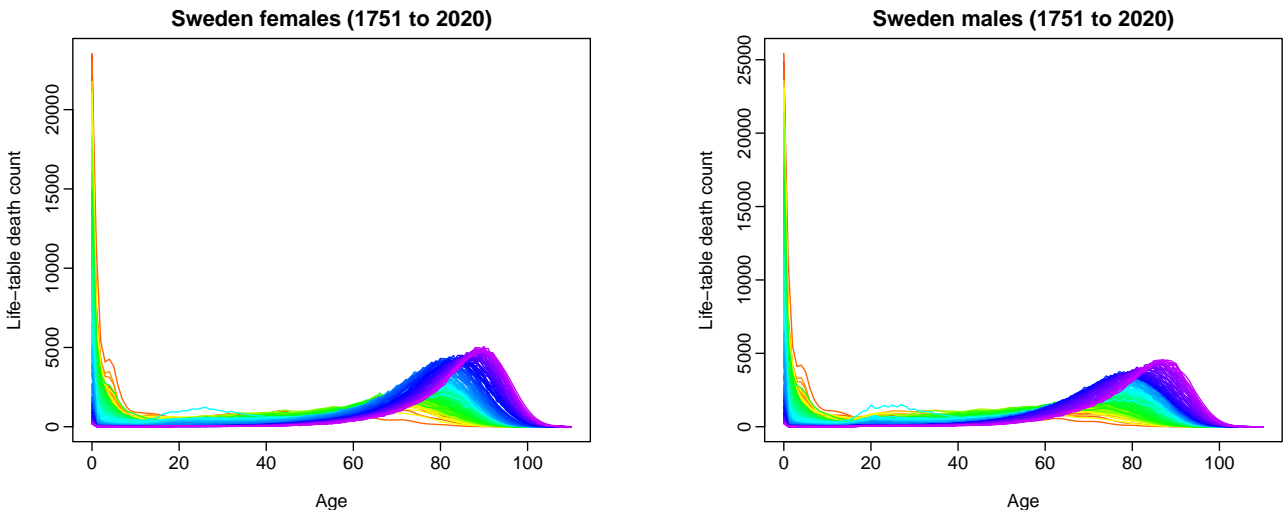


Figure 1 Rainbow plots of age-specific period life-table death count from 1751 to 2020 in a single-year group in Sweden. Curves are ordered chronologically according to the colors of the rainbow. The oldest years are displayed in red, with the most recent years shown in violet.

Both sub-figures demonstrate a slowly decreasing trend in infant death counts and a typical negatively skewed distribution for the life-table death counts, where the peaks shift to higher ages for both females and males. This gradual shift is a primary driver of longevity risk, which is a major issue for insurers and pension funds, especially in the selling and risk management of annuity products (see [Denuit et al. 2007](#), for a discussion).

The re-distribution of life-table death counts indicates lifespan variability across ages. A decrease in variability over time can be observed. This variability can be measured, for example, with the interquartile range of life-table death counts or the Gini coefficient (for comprehensive reviews, see [Wilmoth & Horiuchi 1999](#), [Shkolnikov et al. 2003](#), [van Raalte & Caswell 2013](#), [Debón et al. 2017](#)). In economics, the Gini coefficient summarizes the degree of concentration contained in the Lorenz curve with a single value, and its value varies from 0 (perfect equality) to 1 (perfect inequality). Since income and death counts are inversely related, a value of 0 indicates perfect inequality among ages in life-table death counts, and a value of 1 indicates perfect equality, implying that death occurs at the same age.

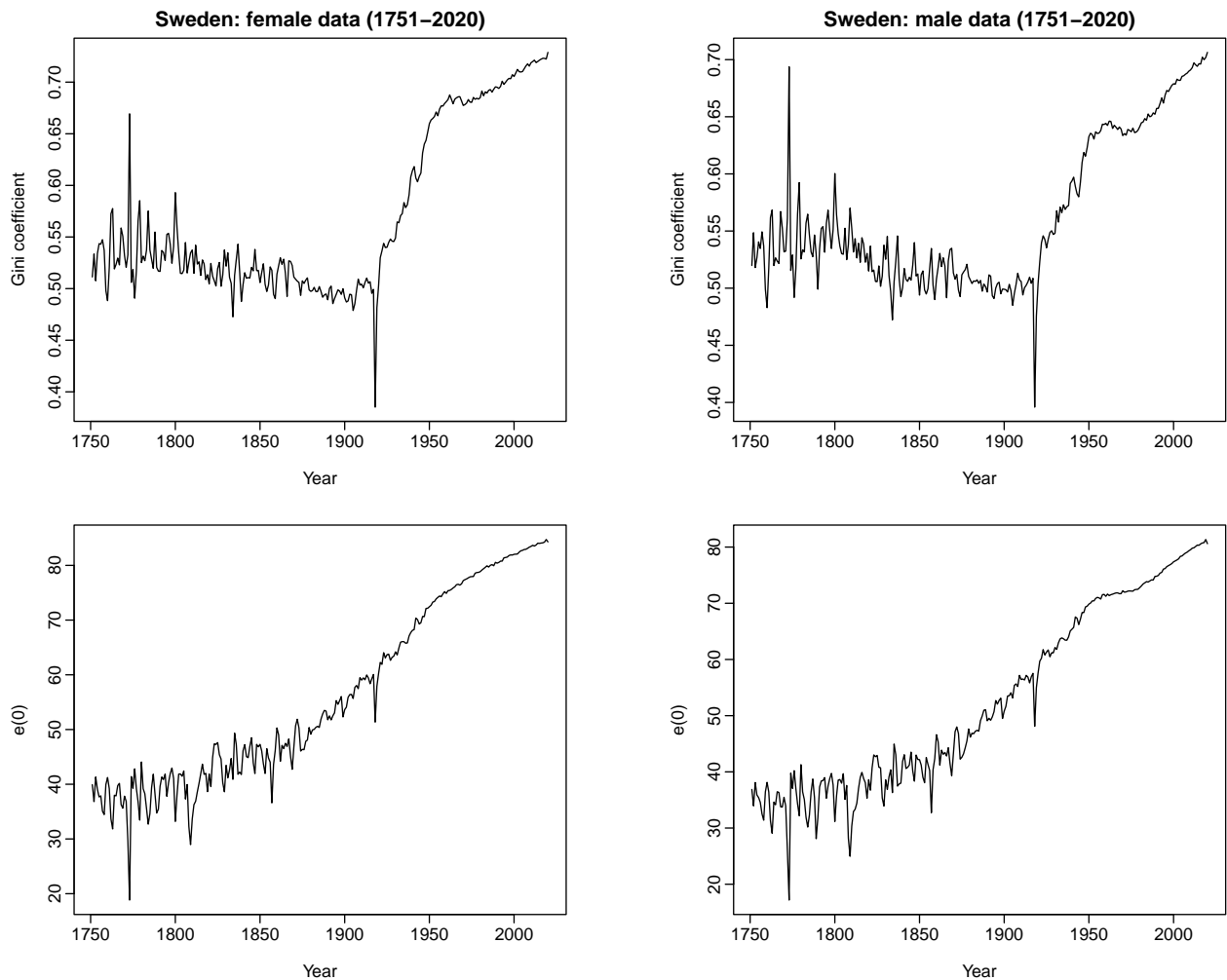


Figure 2 Gini coefficients and life expectancy at age 0, $e(0)$, for Swedish period female and male life-table death counts from 1751 to 2020. When the Gini coefficient approaches 0, it indicates perfect inequality across ages in the life-table death counts. When the Gini coefficient approaches 1, it indicates perfect equality.

Figure 2 presents an example where the life-table death counts provide essential insights into longevity and lifespan variability that cannot be grasped directly from examining the trend in the age-specific central mortality rate or the survival function. We also include graphs of the trend in life expectancy at age zero, denoted by $e(0)$, over time.

The Gini coefficient can be viewed as a single summary measure of inequality in a distribution. In economics, it is derived from the Lorenz curve which is non-decreasing. The Lorenz curve shares a strong resemblance to a cumulative distribution function. In economics, denote p as the fraction of the population that holds $L(p)$ proportion of the whole income. The Gini coefficient can then be expressed as

$$G = 2 \int_0^1 [p - L(p)] dp.$$

The distribution of death counts has an inverse relationship to the income. When the coefficient equals 0, it expresses maximal age-at-death inequality. Inversely, when the coefficient equals 1, equality occurs for all ages. From Figure 2, the effects of the cholera epidemic that occurred in 1834 are apparent for the Swedish female and male data (Larsson 2020). In 1918, there was a sudden drop in the Gini coefficient related to the Spanish flu pandemic.

3 Geometrically weighted compositional data analytic approach

Density functions are non-negative functions that integrate into one. They share features with compositional data (see, e.g., Aitchison 1986, Pawlowsky-Glahn et al. 2015). Compositional data arise in many scientific fields, such as geology (geochemical elements), economics (income/expenditure distribution), medicine (body composition), the food industry (food composition), chemistry (chemical composition), agriculture (nutrient balance bionomics), environmental science (soil contamination), ecology (abundance of different species) and demography (life-table death counts).

In statistics, Scealy et al. (2017) uses CoDa to study the concentration of chemical elements in sediment. Scealy & Welsh (2017) apply CoDa to analyze the total weekly household expenditure on food and housing costs. Delicado (2011), Kokoszka et al. (2019), Shang & Haberman (2020), and Shang et al. (2022) use the centered log-ratio transformation to analyze density functions and implement principal component analysis on the unconstrained space. In demography, Oeppen (2008) and Bergeron-Boucher et al. (2017) introduce a principal component analysis approach to forecast life-table death counts within the centered log-ratio transformation.

For a given year t , compositional data are defined as a random vector of I non-negative components, $[d_t(u_1), \dots, d_t(u_I)]$, whose sum is a specified constant, such as one (portion), 100 (percentage), 10^5 (radix) in life-table death counts, and 10^6 (parts per million) in geochemical trace element compositions (Aitchison 1986, p.1). Between the non-negativity and summability

constraints, the sample space of compositional data is a simplex:

$$\mathcal{S}^I = \left\{ [d_t(u_1), \dots, d_t(u_I)]^\top, \quad d_t(u_i) > 0, \quad \sum_{i=1}^I d_t(u_i) = c \right\}, \quad t = 1, \dots, n,$$

where u denotes a continuum, such as age in this study, c is a fixed constant, $^\top$ denotes vector transpose, and \mathcal{S} denotes a simplex. The simplex sample space is a $I - 1$ dimensional subset of the real-valued space R^I . The restriction of shares to the unit simplex sometimes leads to the lack of an interpretable covariance structure, which has been recognized by researchers in many fields (see, e.g., [Aitchison 1986](#), [Barceló et al. 1996](#), [Fry et al. 1996](#)).

The centered log-ratio transformation presents one of many possible ways to deal with the non-negativity constraint by transforming the raw data. The clr transformation (see, e.g., [Aitchison & Shen 1980](#), [Aitchison 1982, 1986](#)) is a mapping between the simplex to the hyperplane in the Euclidean space. PCA can be applied directly to this hyperplane. The algorithm for implementing the weighted CoDa method consists of the following steps:

- 1) Compute the geometric mean function with geometrically decaying weights. The mean function can be estimated by a weighted average

$$\alpha_n(u) = \exp \left\{ \sum_{t=1}^n w_t \ln[d_t(u)] \right\}, \quad (1)$$

where $w_t = \kappa(1 - \kappa)^{n-t}$ is a set of geometrically decaying weights with $0 < \kappa < 1$ and $\sum_{t=1}^n w_t = 1$, $\ln(\cdot)$ denotes natural logarithm, and $d_t(u) > 0$ denotes the age-specific life-table death count (see Section 2 for the treatment of $d_t(u) = 0$). In Figure 3, we display geometrically decaying weights when the weight parameter $\kappa = 0.05$ or 0.95 , respectively. When $\kappa = 0.05$, forecasts depend on more distant past observations. When $\kappa = 0.95$, forecasts rely on the most recent observations.

We treat age as a continuum $u \in [0, 110]$ although age is observed at discrete points and set

$$s_t(u) = \frac{d_t(u)}{\alpha_n(u)}. \quad (2)$$

- 2) Apply the centered log-ratio transformation given by

$$\beta_t(u) = \ln[s_t(u)]$$

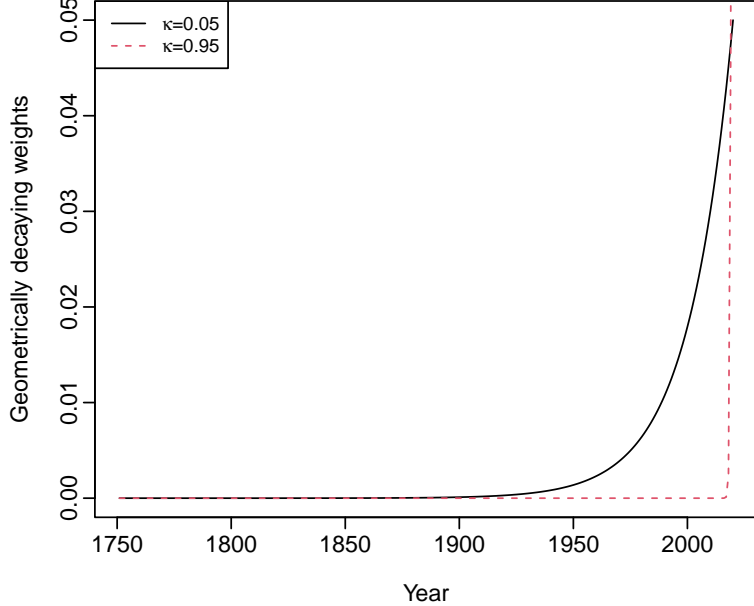


Figure 3 Geometrically decaying weights when $\kappa = 0.05$ and 0.95 , respectively.

From (1) and (2), we obtain

$$\begin{aligned}\beta_t(u) &= \ln d_t(u) - \ln \alpha_n(u) \\ &= \ln d_t(u) - \sum_{t=1}^n w_t \ln d_t(u)\end{aligned}$$

For a given population, $\beta_t(u)$ can be viewed as an unconstrained functional time series.

3) Compute eigenvalues and eigenfunctions from the covariance across t of the weighted unconstrained functional time series: Let $\beta(u) = [\beta_1(u), \dots, \beta_n(u)]^\top$ be a time series of unconstrained functions, and $\mathbf{w} = \text{diagonal}(w_1, \dots, w_n)$. The weighted curve time series is given as $\beta^*(u) = \mathbf{w}\beta(u)$. The weighting scheme aims to help find the most suitable basis functions for the curve time series to project onto. Applying eigendecomposition to $\beta^*(u)$ gives

$$\beta_t^*(u) = \sum_{k=1}^n \hat{\gamma}_{t,k} \hat{\phi}_k(u) = \sum_{k=1}^K \hat{\gamma}_{t,k} \hat{\phi}_k(u) + \omega_t(u), \quad (3)$$

where $\hat{\phi}_k(u)$ is the k^{th} weighted orthonormal eigen-function (i.e., functional principal components), $\hat{\gamma}_{t,k} = \langle \beta_t(u), \hat{\phi}_k(u) \rangle$ is the k^{th} set of principal component scores at time t , and $\omega_t(u)$ denotes the model residual function for age u in year t .

When $K = 1$, (3) reduces to the a version of the [Lee & Carter's \(1992\)](#) method. The Lee-Carter model estimates parameters by minimizing the residual sum of squares via singular value decomposition. While the Lee-Carter model has the advantage of being nonparametric, its goodness-of-fit and forecasting performance can be improved with the inclusion of higher-

order principal components (see, e.g., [Brouhns et al. 2002](#), [Renshaw & Haberman 2003](#), [Booth & Tickle 2008](#)). We consider an eigenvalue ratio criterion of [Li et al. \(2020\)](#) to select the optimal value of K , and $K = 6$ as used in [Hyndman et al. \(2013\)](#) and the default opinion in the demography package ([Hyndman 2023](#)).

4) *Forecasting $\beta^*(u)$.* By conditioning on the estimated functional principal components $\Phi(u) = [\hat{\phi}_1(u), \dots, \hat{\phi}_K(u)]$ and observed data $\beta^*(u)$, the h -step-ahead forecast of $\beta^*(u)$ can be obtained

$$\hat{\beta}_{n+h|n}^*(u) = E[\beta_{n+h}(u) | \Phi(u), \beta^*(u)] = \sum_{k=1}^K \hat{\gamma}_{n+h|n,k} \hat{\phi}_k(u),$$

where $\hat{\gamma}_{n+h|n,k}$ denotes the h -step-ahead univariate time-series forecast of the k^{th} set of principal component scores. Among univariate time-series methods, we consider the random walk with drift (RWD) method for forecasting principal component scores.

5) *Transform back to the compositional data.* We take the inverse centered log-ratio transformation given by

$$\hat{s}_{n+h|n}(u) = \left[\exp^{\hat{\beta}_{n+h|n}^*(u_1)}, \exp^{\hat{\beta}_{n+h|n}^*(u_2)}, \dots, \exp^{\hat{\beta}_{n+h|n}^*(u_{111})} \right],$$

where $\hat{\beta}_{n+h|n}^*(u_i)$ denotes the forecasts in Step 3).

6) We add back the geometric means to obtain the life-table death count forecasts $\hat{d}_{n+h}(u)$,

$$\hat{d}_{n+h|n}(u) = \left[\hat{s}_{n+h|n}(u_1) \times \alpha_n(u_1), \hat{s}_{n+h|n}(u_2) \times \alpha_n(u_2), \dots, \hat{s}_{n+h|n}(u_{111}) \times \alpha_n(u_{111}) \right]$$

where $\alpha_n(u_i)$ is the weighted geometric mean given in Step 1).

To evaluate forecast uncertainty, we apply a nonparametric bootstrap method to generate future sample paths. We consider two sources of uncertainty: truncation errors in the functional principal component decomposition and forecast errors in the predicted principal component scores (see, e.g., [Hyndman & Shang 2009](#), [Shang & Haberman 2020](#)). Since principal component scores are regarded as surrogates of the original functional time series, these principal component scores capture the temporal dependence structure inherited in the original functional time series (see, e.g., [Paparoditis 2018](#), [Shang 2018](#), [Paparoditis & Shang 2023](#)). By adequately bootstrapping the forecast principal component scores, we can generate a set of bootstrapped forecasts $\hat{\beta}_{n+h|n}^*(u) = [\hat{\beta}_{n+h|n}^{(1)}(u), \dots, \hat{\beta}_{n+h|n}^{(B)}(u)]$, conditional on the estimated weighted mean function and weighted functional principal components from the observed data.

Using a univariate time series model, we can obtain multi-step-ahead forecasts for the principal component scores, $\{\hat{\gamma}_{1,k}, \dots, \hat{\gamma}_{n,k}\}$ for $k = 1, \dots, K$. Let the h -step-ahead forecast errors be given by $\vartheta_{t,h,k} = \hat{\gamma}_{t,k} - \hat{\gamma}_{t|t-h,k}$ for $t = h + 1, \dots, n$. The forecast errors, $\vartheta_{t,h,k}$, measure the difference

between the estimated and forecast principal component scores. These can then be sampled with replacement to give a bootstrap sample for $\gamma_{n+h,k}$:

$$\widehat{\gamma}_{n+h|n,k}^{(b)} = \widehat{\gamma}_{n+h|n,k} + \vartheta_{*,h,k}^{(b)}, \quad b = 1, \dots, B,$$

where $B = 1,000$ symbolizes the number of bootstrap samples and $\vartheta_{*,h,k}^{(b)}$ are sampled with replacement from $\{\vartheta_{h+1,h,k}, \dots, \vartheta_{n,h,k}\}$.

Assuming the first K functional principal components approximate the original functional time series relatively well, the model residuals should contribute nothing but random noise. In contrast to the underestimation of K , the overestimation of K does not hinder much forecast accuracy (see also [Hyndman et al. 2013](#)). Consequently, we can bootstrap the model fit errors in (3) by sampling with replacement from the model residual term $\{\omega_1(u), \dots, \omega_n(u)\}$.

Due to orthonormality, these two components of variability are summable. We obtain B variants of $\beta_{n+h}(u)$,

$$\widehat{\beta}_{n+h|n}^{(b)}(u) = \sum_{k=1}^K \widehat{\gamma}_{n+h|n,k}^{(b)} \widehat{\phi}_k(u) + \omega_{n+h}^{(b)}(u),$$

where $\widehat{\gamma}_{n+h|n,k}^{(b)}$ denotes the bootstrap forecast of the principal component scores.

With the bootstrapped $\widehat{\beta}_{n+h|n}^{*}(u)$, we follow Steps 4) and 5) of the above algorithm to obtain the bootstrap forecasts of $d_{n+h|n}^{*}(u)$. At the $100(1 - \alpha)\%$ nominal coverage probability, the pointwise prediction intervals are obtained by taking $\alpha/2$ and $1 - \alpha/2$ quantiles based on $\{\widehat{d}_{n+h|n}^{(1)}(u), \dots, \widehat{d}_{n+h|n}^{(B)}(u)\}$.

4 Selection of the geometrically decaying weight parameter

4.1 Point forecast error criteria

Since the age-specific life-table death counts can be considered a probability density function, we also consider density evaluation metrics. They include discrete Kullback-Leibler divergence ([Kullback & Leibler 1951](#)) and the square root of the Jensen-Shannon divergence ([Shannon 1948](#), [Fuglede & Topsoe 2004](#)).

The Kullback-Leibler divergence measures information loss by replacing an unknown density with an approximation. For two probability density functions, denoted by $d_{n+\xi}(u)$ and $\widehat{d}_{n+\xi|n}(u)$,

the discrete Kullback-Leibler divergence is defined as

$$\begin{aligned}
\text{KLD}(h) &= D_{\text{KL}}[d_{n+\xi}(u_i) \parallel \widehat{d}_{n+\xi|n}(u_i)] + D_{\text{KL}}[\widehat{d}_{n+\xi|n}(u_i) \parallel d_{n+\xi}(u_i)] \\
&= \frac{1}{111 \times (11-h)} \sum_{\xi=h}^{10} \sum_{i=1}^{111} d_{n+\xi}(u_i) \cdot [\ln d_{n+\xi}(u_i) - \ln \widehat{d}_{n+\xi|n}(u_i)] + \\
&\quad \frac{1}{111 \times (11-h)} \sum_{\xi=h}^{10} \sum_{i=1}^{111} \widehat{d}_{n+\xi|n}(u_i) \cdot [\ln \widehat{d}_{n+\xi|n}(u_i) - \ln d_{n+\xi}(u_i)],
\end{aligned}$$

where $i = 111$ corresponds to the number of age groups, and ξ corresponds to the forecasting period. The discrete Kullback-Leibler divergence is symmetric and non-negative.

An alternative is given by the Jensen-Shannon divergence, defined by

$$\text{JSD}(h) = \frac{1}{2} D_{\text{KL}}[d_{n+\xi}(u_i) \parallel \delta_{n+\xi}(u_i)] + \frac{1}{2} D_{\text{KL}}[\widehat{d}_{n+\xi|n}(u_i) \parallel \delta_{n+\xi}(u_i)],$$

where $\delta_{n+\xi}(u_i)$ measures a common quantity between $d_{n+\xi}(u_i)$ and $\widehat{d}_{n+\xi|n}(u_i)$. We consider the simple mean $\delta_{n+\xi}(u_i) = \frac{1}{2}[d_{n+\xi}(u_i) + \widehat{d}_{n+\xi|n}(u_i)]$ or geometric mean $\delta_{n+\xi}(u_i) = \sqrt{d_{n+\xi}(u_i) \widehat{d}_{n+\xi|n}(u_i)}$. We denote $\text{JSD}^s(h)$ for the Jensen-Shannon divergence with the simple mean and $\text{JSD}^g(h)$ for the Jensen-Shannon divergence with the geometric mean.

4.2 Interval forecast error criteria

To evaluate the interval forecast accuracy, we consider the coverage probability difference (CPD) between the empirical and nominal coverage probabilities. For each year in the forecasting period, the h -step-ahead prediction intervals are computed at the $100(1 - \nu)\%$ nominal coverage probability, where ν denotes a significance level, such as $\nu = 0.2$ or 0.05 . We consider the common case of the symmetric $100(1 - \nu)\%$ prediction intervals, with lower and upper bounds that are predictive quantiles at $\nu/2$ and $1 - \nu/2$, denoted by $\widehat{d}_{n+\xi}^{\text{lb}}(u_i)$ and $\widehat{d}_{n+\xi}^{\text{ub}}(u_i)$. The empirical coverage probability (ECP) is defined as

$$\text{ECP}(h) = 1 - \frac{1}{111 \times (11-h)} \sum_{\xi=h}^{10} \sum_{i=1}^{111} \left[\mathbb{1}\{d_{n+\xi}(u_i) > \widehat{d}_{n+\xi}^{\text{ub}}(u_i)\} + \mathbb{1}\{d_{n+\xi}(u_i) < \widehat{d}_{n+\xi}^{\text{lb}}(u_i)\} \right].$$

The CPD is then expressed as

$$\text{CPD}(h) = |\text{ECP}(h) - (1 - \nu)|.$$

4.3 Expanding window scheme

An expanding window scheme of a time series model is commonly used to assess model and parameter stability over time and the reliability of predictions. The expanding window analysis determines the variability of the model's parameters by computing parameter estimates and their forecasts over an expanding window. In Figure 4, we visually display sample splitting.

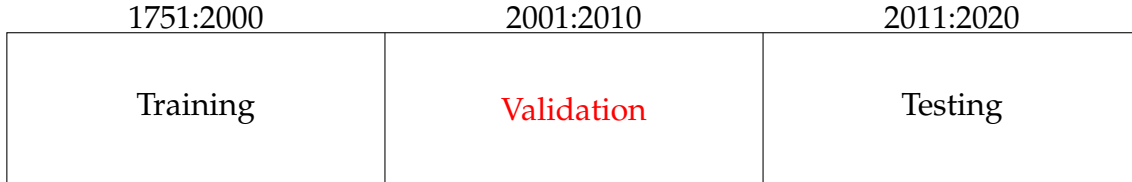


Figure 4 Illustration of the cross-validation method. A model is constructed using data in the training set to forecast data in the validation set. The optimal weight parameter is determined based on the minimal forecast error in the validation set.

Using the first 250 observations from 1751 to 2000 in the life-table death counts, we produce one- to 10-step-ahead forecasts. Through an expanding window approach, we re-estimate the parameters using the first 251 observations from 1751 to 2001. Forecasts from the estimated models are then produced for one- to nine-step-ahead forecasts. We iterated this process by increasing the sample size by one year until we reached the data in 2010. This process produces 10 one-step-ahead forecasts, 9 two-step-ahead forecasts, . . . , and one 10-step-ahead forecast. We compare these forecasts with the validation samples from 2001 to 2010 to determine the optimal weight parameter, κ , for each of the ten forecast horizons. In Table 1, we tabulate the estimated geometrically decaying weight parameters in the weighted CoDa method under the KLD and two variants of the JSD.

Table 1 Estimated geometrically decaying weight parameters in the weighted CoDa method under the KLD and two variants of the JSD. The values in bold are used in our demonstration in Figure 5. The number of retained functional principal components is $K = 6$ as used in [Hyndman et al. \(2013\)](#).

h	Female			Male		
	KLD	JSD ^s	JSD ^g	KLD	JSD ^s	JSD ^g
1	0.024	0.024	0.024	0.016	0.016	0.021
2	0.024	0.024	0.024	0.019	0.029	0.029
3	0.049	0.049	0.025	0.029	0.019	0.019
4	0.052	0.053	0.052	0.076	0.076	0.076
5	0.055	0.055	0.055	0.019	0.019	0.080
6	0.054	0.025	0.025	0.030	0.030	0.030
7	0.056	0.056	0.056	0.094	0.094	0.094
8	0.059	0.060	0.059	0.093	0.093	0.093
9	0.064	0.065	0.065	0.104	0.105	0.104
10	0.055	0.003	0.000	0.106	0.106	0.106

4.4 CoDa model fitting

We apply the standard and weighted CoDa methods to the Swedish female and male data. From the observed life-table death counts from 1751 to 2019 (i.e., 278 observations), we present the simple and weighted geometric means of the female and male life-table death counts in Figures 5a and 5b. The estimated functions for the standard CoDa method are shown in red, while those for the weighted CoDa method are displayed in blue. Via functional principal component analysis, we display the first estimated functional principal component in Figures 5c and 5d.

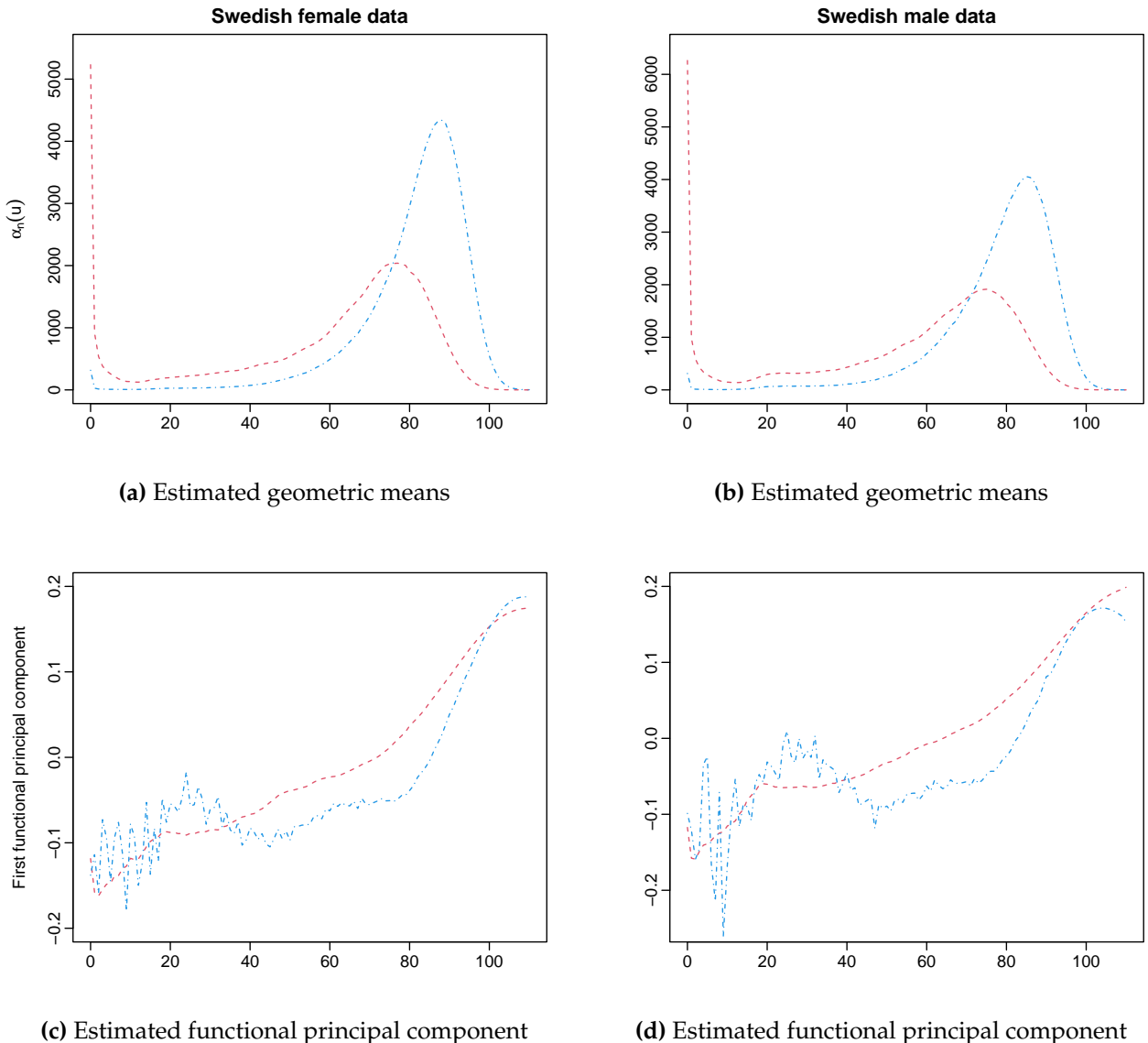
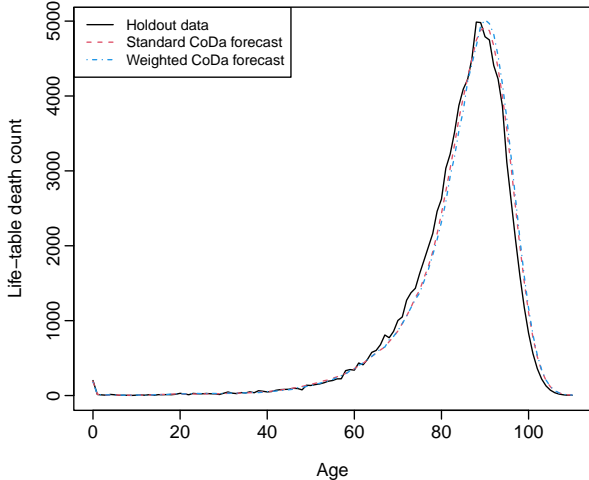
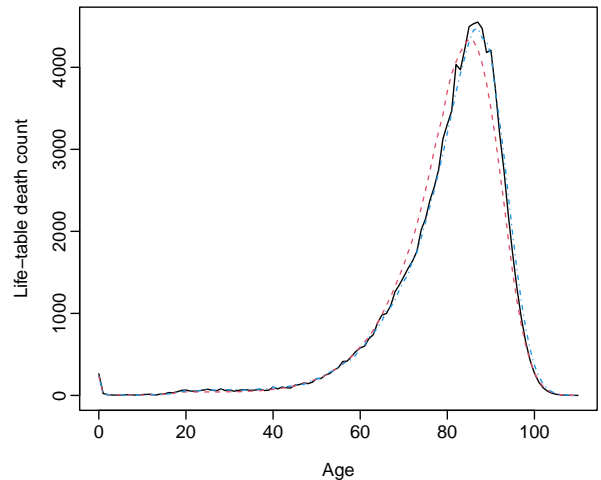


Figure 5 Elements of the CoDa methods for modeling and forecasting the Swedish female and male life-table death counts. The estimated functions for the standard CoDa method are shown in red, while the estimated functions for the weighted CoDa method are displayed in blue.

For producing one-step-ahead forecasts, the weight parameters $\kappa = 0.024$ and 0.016 are based on the KLD, as shown in Table 1. From the one-step-ahead point forecasts of life-table death counts in 2020, the weighted CoDa method produces one-step-ahead forecasts that are comparably closer to the holdout data as shown in Figures 6a and 6b.



(a) One-step-ahead forecast life-table death counts



(b) One-step-ahead forecast life-table death counts

Figure 6 One-step-ahead forecasts between the CoDa method shown in red and the weighted CoDa method in blue.

5 Comparison of point forecast accuracy

Using the first 260 observations from 1751 to 2010, we produce one- to 10-step-ahead forecasts via an expanding window approach. We evaluate forecast accuracy by comparing the forecasts with the holdout data from 2011 to 2020. Table 2 presents point forecast evaluation metrics between standard and geometrically decaying weighted CoDa methods for the Swedish female and male data. The weighted CoDa method's estimated weight parameters for different horizons are tabulated in Table 1. For the CoDa method, we consider using the fitting period from 1950 onwards and all available data.

Table 2 Comparison of point forecast errors ($\times 100$), namely the KLD and two variants of the JSD, between the CoDa and its weighted variant for forecasting the age-specific Swedish female and male data. Based on the averages of the point forecast errors, minimum values are highlighted in bold. The eigenvalue ratio criterion is shorted as the EVR.

Sex	K	h	CoDa			CoDa (1950)			Weighted CoDa		
			KLD	JSD ^s	JSD ^g	KLD	JSD ^s	JSD ^g	KLD	JSD ^s	JSD ^g
Female	EVR	1	1.278	0.314	0.315	0.207	0.049	0.049	0.185	0.043	0.043
		2	1.353	0.333	0.334	0.183	0.043	0.043	0.162	0.037	0.037
		3	1.448	0.356	0.358	0.199	0.046	0.047	0.171	0.039	0.040
		4	1.519	0.373	0.375	0.206	0.048	0.048	0.163	0.036	0.037
		5	1.519	0.373	0.375	0.247	0.058	0.058	0.206	0.047	0.048
		6	1.585	0.390	0.392	0.300	0.071	0.072	0.210	0.050	0.050
		7	1.683	0.414	0.417	0.357	0.086	0.086	0.226	0.053	0.053
		8	1.835	0.452	0.455	0.330	0.079	0.079	0.265	0.062	0.063
		9	1.886	0.464	0.468	0.431	0.104	0.105	0.299	0.070	0.071
		10	1.170	0.288	0.289	0.840	0.205	0.206	0.220	0.051	0.051

Continued on next page

Sex	K	h	KLD	JSD ^s	JSD ^g	KLD	JSD ^s	JSD ^g	KLD	JSD ^s	JSD ^g
		Mean	1.527	0.376	0.378	0.330	0.079	0.079	0.211	0.049	0.049
K = 6	1	1	0.282	0.067	0.067	0.212	0.048	0.049	0.248	0.057	0.057
		2	0.309	0.073	0.074	0.198	0.044	0.045	0.232	0.052	0.052
		3	0.324	0.078	0.078	0.220	0.050	0.050	0.206	0.045	0.049
		4	0.362	0.087	0.087	0.237	0.054	0.055	0.229	0.051	0.052
		5	0.373	0.089	0.089	0.289	0.066	0.067	0.230	0.050	0.051
		6	0.458	0.111	0.112	0.364	0.086	0.087	0.270	0.069	0.069
		7	0.615	0.150	0.151	0.444	0.106	0.107	0.316	0.074	0.074
		8	0.645	0.158	0.158	0.438	0.104	0.105	0.281	0.065	0.065
		9	0.655	0.160	0.161	0.537	0.128	0.128	0.365	0.084	0.085
		10	0.300	0.072	0.072	1.001	0.243	0.243	0.215	0.086	0.088
		Mean	0.432	0.104	0.105	0.394	0.093	0.093	0.259	0.063	0.064
Male	EVR	1	1.246	0.308	0.309	0.643	0.157	0.158	0.242	0.057	0.058
		2	1.392	0.344	0.345	0.687	0.168	0.169	0.228	0.054	0.054
		3	1.510	0.374	0.375	0.701	0.172	0.172	0.214	0.050	0.051
		4	1.632	0.403	0.405	0.757	0.185	0.186	0.301	0.071	0.072
		5	1.719	0.425	0.427	0.753	0.184	0.185	0.265	0.063	0.063
		6	1.908	0.472	0.474	0.901	0.221	0.221	0.410	0.098	0.098
		7	2.112	0.523	0.525	0.994	0.244	0.245	0.470	0.114	0.114
		8	2.115	0.524	0.526	0.905	0.222	0.222	0.434	0.105	0.105
		9	2.077	0.514	0.516	0.849	0.207	0.208	0.454	0.109	0.109
		10	1.250	0.309	0.309	0.552	0.131	0.132	0.187	0.044	0.044
		Mean	1.696	0.419	0.421	0.774	0.189	0.190	0.321	0.076	0.077
K = 6	1	1	0.231	0.055	0.055	0.251	0.059	0.059	0.233	0.054	0.053
		2	0.241	0.057	0.058	0.249	0.058	0.058	0.220	0.051	0.051
		3	0.203	0.048	0.048	0.266	0.062	0.063	0.260	0.059	0.059
		4	0.262	0.062	0.063	0.312	0.073	0.073	0.331	0.077	0.078
		5	0.269	0.064	0.065	0.271	0.064	0.064	0.322	0.077	0.074
		6	0.355	0.085	0.086	0.423	0.100	0.101	0.480	0.114	0.114
		7	0.420	0.102	0.102	0.370	0.088	0.088	0.506	0.121	0.122
		8	0.401	0.097	0.098	0.378	0.090	0.090	0.518	0.124	0.125
		9	0.438	0.106	0.106	0.484	0.115	0.115	0.653	0.155	0.156
		10	0.223	0.053	0.053	0.293	0.067	0.068	0.288	0.067	0.067
		Mean	0.304	0.073	0.073	0.330	0.077	0.078	0.381	0.090	0.090

For forecasting the Swedish female life-table death counts, we observe 1) The CoDa method with the fitting period from 1950 onwards produces more accurate point forecasts than the one with all available data in the fitting period. 2) From a forecast accuracy perspective, it is advantageous to use $K = 6$, compared with the eigenvalue ratio criterion. 3) Based on the averaged error criterion, the weighted CoDa method generally produces more accurate forecasts than the standard CoDa method. When $h = 1, 2$, we also show that the CoDa method with the fitting period from 1950 onwards can outperform the weighted CoDa method.

For forecasting the Swedish male life-table death counts, we observe 1) The CoDa method with

a longer fitting period produces more accurate point forecasts than the one from 1950 onwards. 2) The weighted CoDa method produces more accurate point forecasts for shorter horizons rather than at longer horizons. 3) From a forecast accuracy perspective, it is advantageous to use $K = 6$, compared with the eigenvalue ratio criterion. Hereafter, we report the results based on $K = 6$.

6 Comparison of interval forecast accuracy

In Table 3, we tabulate the estimated weight parameter in the weighted CoDa method under the CPD metrics. Notably, the selected weight parameters all lie between 0.051 and 0.147. Using the selected weight parameters in Table 3, we present interval forecast accuracy between the standard and weighted CoDa methods for the Swedish data.

Table 3 Estimated geometrically decaying weight parameters in the weighted CoDa method under the CPD.

h	Female		Male	
	$\alpha = 0.2$	0.05	0.2	0.05
1	0.075	0.061	0.083	0.106
2	0.083	0.090	0.100	0.136
3	0.085	0.089	0.100	0.117
4	0.081	0.093	0.108	0.100
5	0.084	0.087	0.108	0.137
6	0.078	0.100	0.126	0.100
7	0.083	0.086	0.114	0.142
8	0.086	0.091	0.100	0.102
9	0.076	0.051	0.100	0.100
10	0.100	0.100	0.147	0.100

As shown in Table 4, the weighted CoDa method produces smaller CPD values than those obtained from the standard CoDa methods at $\alpha = 0.05$. For $\alpha = 0.2$, the CoDa method with the fitting period from 1950 performs the best.

Table 4 Comparison of the CPD between the CoDa and its weighted variant for forecasting the age-specific Swedish data.

K	h	CoDa		CoDa (1950)		Weighted CoDa	
		$\alpha = 0.2$	$\alpha = 0.05$	$\alpha = 0.2$	$\alpha = 0.05$	$\alpha = 0.2$	$\alpha = 0.05$
Female	1	0.167	0.046	0.030	0.035	0.053	0.007
	2	0.180	0.050	0.034	0.027	0.054	0.034
	3	0.188	0.049	0.045	0.041	0.038	0.025
	4	0.187	0.050	0.012	0.048	0.023	0.032
	5	0.183	0.050	0.054	0.037	0.030	0.015
	6	0.195	0.050	0.058	0.040	0.022	0.027

7	0.195	0.050	0.034	0.015	0.012	0.014
8	0.194	0.050	0.070	0.013	0.029	0.008
9	0.186	0.050	0.088	0.004	0.007	0.023
10	0.191	0.050	0.011	0.004	0.178	0.049
	Mean	0.187	0.050	0.044	0.026	0.045
Male	1	0.191	0.050	0.005	0.028	0.083
	2	0.188	0.049	0.016	0.046	0.080
	3	0.195	0.050	0.045	0.022	0.057
	4	0.195	0.049	0.072	0.041	0.059
	5	0.195	0.050	0.009	0.025	0.036
	6	0.196	0.050	0.085	0.049	0.086
	7	0.195	0.050	0.041	0.047	0.036
	8	0.194	0.050	0.028	0.013	0.044
	9	0.200	0.050	0.057	0.049	0.025
	10	0.191	0.050	0.074	0.023	0.106
	Mean	0.194	0.050	0.043	0.034	0.061

7 Application to a single-premium temporary immediate annuity

An important use of mortality forecasts for individuals over 60 is in the pension and insurance industries, whose profitability and solvency depend on accurate mortality forecasts to hedge longevity risk. Longevity risk is the chance that life expectancies exceed expectations for pricing, resulting in greater than anticipated cash flow needs from insurance companies or pension funds. When a person retires, an optimal way of guaranteeing one individual's financial income in retirement is to purchase an annuity (see [Yaari 1965](#)). An annuity is a financial contract offered by insurers that guarantees a steady stream of income for a temporary or lifetime of the annuitants in exchange for an initial premium charge.

Following [Shang & Haberman \(2017\)](#), we consider temporary annuities, which have grown in popularity in many developed countries, because immediate lifetime annuities, where rates are locked in for life, have been shown to deliver poor value for money (see [Cannon & Tonks 2008](#), Chapter 6). These temporary annuities pay a pre-determined and guaranteed income level higher than the income provided by a lifetime annuity for a similar premium. Fixed-term annuities offer a more affordable alternative to lifetime annuities and allow the purchaser to purchase a deferred annuity to address the tail longevity risk.

We obtain forecasts of life-table death counts using the standard and weighted CoDa methods and then determine the corresponding survival probabilities. Using the RWD forecasting method, we display the forecasts of the life-table death counts from 2021 to 2070 for Swedish females and males in Figure 7.

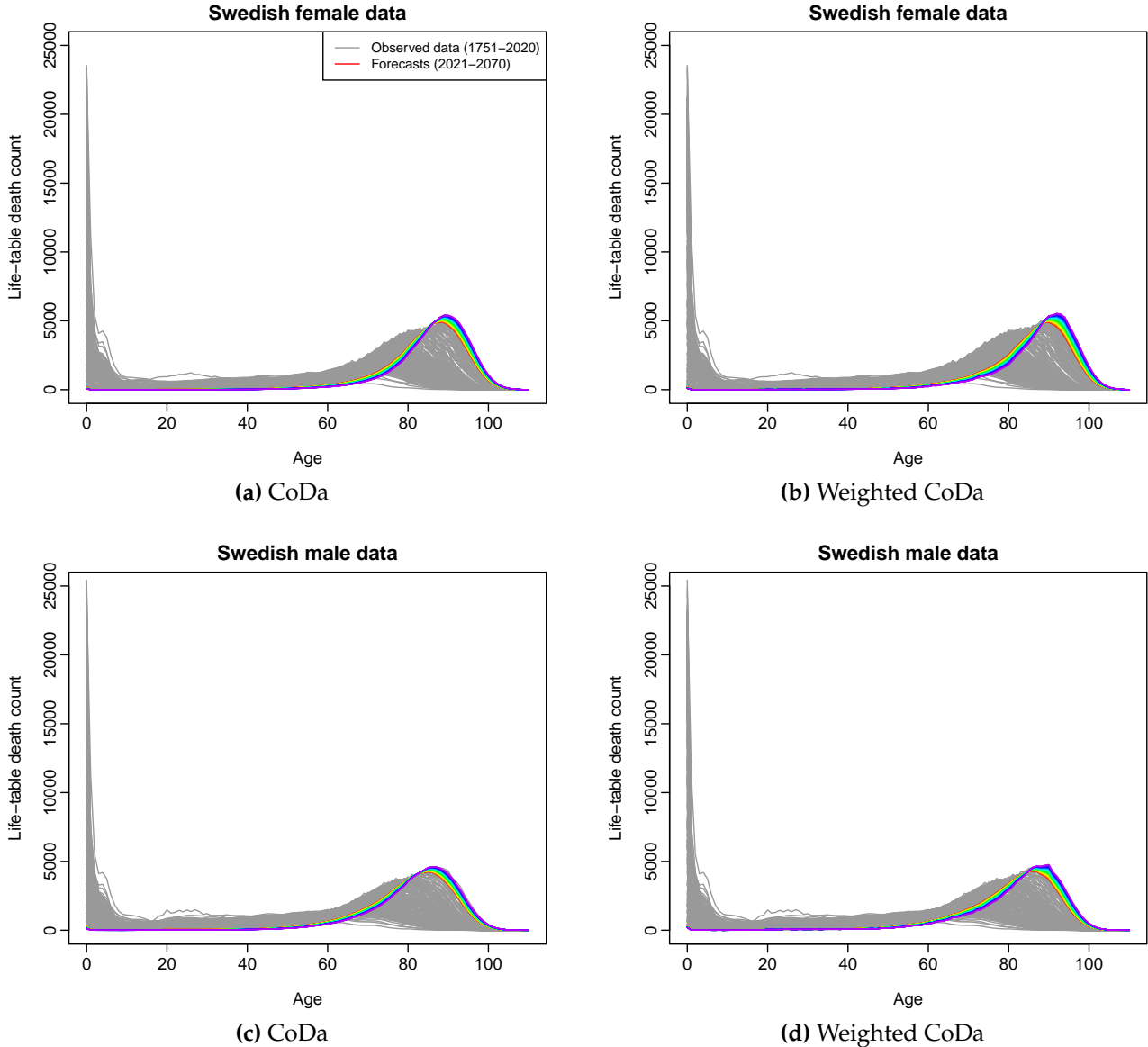


Figure 7 Age-specific life-table death count point forecasts from 2021 to 2070 for Swedish females and males.

With the forecasts of the life-table death counts, we compute a single-premium temporary immediate annuity (see [Dickson et al. 2009](#), p.114), and we adopt a cohort approach to the computation of the survival probabilities. The τ year survival probability of a person aged x at $t = 0$ (or year x) is determined by

$$\tau p_x = \prod_{x=0}^{\tau-1} p_x = \prod_{x=1}^{\tau-1} (1 - q_x) = \prod_{x=1}^{\tau-1} \left(1 - \frac{d_x}{l_x}\right),$$

where d_x denotes the number of death counts between two successive ages x and $x + 1$, and l_x denotes the number of lives alive at age x .

Annuity price with a maturity period of T year is a random quantity, which depends on the value of zero-coupon bond price and future mortality. For an x -year-old with benefits \$1 per year,

the temporary immediate annuity price can be written as

$$a_x^T = \sum_{\tau=1}^T B(0, \tau) \tau p_x,$$

where $B(0, \tau)$ is the τ -year bond price and τp_x denotes the survival probability.

In Table 5, we compute our best estimate of annuity prices for various ages and maturities for female and male policyholders residing in Sweden. We assume a constant interest rate at $\zeta = 3\%$ and a zero-coupon bond is given as

$$B(0, \tau) = \exp^{-\zeta \tau}.$$

Table 5 Estimates of annuity prices with various ages and maturities (T) for female and male policyholders residing in Sweden, when the interest rate is set at 3%.

Age	CoDa						Weighted CoDa					
	$T = 5$	10	15	20	25	30	5	10	15	20	25	30
Female												
60	4.517	8.289	11.385	13.844	15.662	16.791	4.515	8.276	11.354	13.785	15.571	16.684
65	4.484	8.165	11.089	13.250	14.592	15.177	4.476	8.139	11.032	13.157	14.482	15.068
70	4.433	7.953	10.555	12.171	12.876	13.045	4.423	7.917	10.484	12.084	12.792	12.967
75	4.334	7.537	9.526	10.394	10.603	10.624	4.319	7.490	9.469	10.343	10.559	10.582
80	4.116	6.673	7.788	8.057	8.084	8.085	4.103	6.662	7.793	8.072	8.102	8.103
85	3.646	5.236	5.619	5.657	5.659		3.665	5.285	5.686	5.728	5.730	
90	2.894	3.590	3.660	3.662			2.921	3.643	3.720	3.723		
95	2.036	2.241	2.248				2.079	2.300	2.309			
100	1.323	1.370					1.359	1.412				
105	0.875						0.907					
Male												
60	4.485	8.161	11.082	13.278	14.742	15.502	4.486	8.166	11.097	13.305	14.782	15.554
65	4.427	7.946	10.591	12.354	13.269	13.569	4.431	7.959	10.617	12.396	13.325	13.631
70	4.339	7.600	9.774	10.903	11.272	11.332	4.344	7.617	9.807	10.952	11.329	11.391
75	4.176	6.959	8.404	8.877	8.953	8.958	4.181	6.979	8.441	8.923	9.002	9.007
80	3.838	5.831	6.483	6.588	6.595	6.595	3.851	5.864	6.527	6.635	6.642	6.642
85	3.249	4.312	4.484	4.495	4.495		3.260	4.334	4.509	4.520	4.520	
90	2.438	2.831	2.856	2.857			2.449	2.846	2.873	2.873		
95	1.671	1.780	1.783				1.680	1.790	1.792			
100	1.110	1.137					1.112	1.139				
105	0.777						0.780					

For the male population, the annuity prices for the weighted CoDa method are higher than the ones produced from the CoDa method. This may indicate the increasing life expectancy for the male population. For the female population, the weighted CoDa method recognizes the longevity

risk trend more than its unweighted counterpart; thus, it produces different mortality forecasts. Between ages 60 and 80, the weighted CoDa mortality forecasts are predicted to be lower than the unweighted counterpart. This implies fewer people are likely to die in that age group. For ages 85 and above, this is a longevity risk group with increasingly more people.

To provide forecast uncertainty, we rely on the bootstrapped life-table death counts, derive the survival probabilities, and compute the associated annuities for different ages and maturities. Since we consider ages from 60 to 110, we construct 50 steps ahead bootstrap forecasts of life-table death counts. In Table 6, we present the 95% pointwise prediction intervals of annuities for different ages and maturities, where $\text{age} + \text{maturity} \leq 110$.

Table 6 Ninety-five percentage pointwise prediction intervals of annuity prices with different ages and maturities (T) for female and male policyholders residing in Sweden, when the interest rate is set at 3%.

Sex	Age	$T = 5$	$T = 10$	$T = 15$	$T = 20$	$T = 25$	$T = 30$
<u>CoDa</u>							
F	60	(4.487, 4.533)	(8.206, 8.338)	(11.235, 11.492)	(13.652, 14.028)	(15.438, 15.951)	(16.556, 17.220)
	65	(4.433, 4.514)	(8.056, 8.254)	(10.913, 11.267)	(13.037, 13.554)	(14.344, 15.073)	(14.924, 15.804)
	70	(4.355, 4.487)	(7.793, 8.114)	(10.329, 10.874)	(11.931, 12.689)	(12.593, 13.584)	(12.769, 13.824)
	75	(4.247, 4.426)	(7.360, 7.817)	(9.333, 10.059)	(10.174, 11.154)	(10.382, 11.435)	(10.409, 11.476)
	80	(3.991, 4.287)	(6.460, 7.167)	(7.516, 8.569)	(7.751, 8.947)	(7.788, 9.000)	(7.789, 9.002)
	85	(3.476, 3.949)	(4.932, 5.940)	(5.284, 6.500)	(5.321, 6.580)	(5.321, 6.583)	
	90	(2.620, 3.399)	(3.203, 4.376)	(3.267, 4.477)	(3.270, 4.490)		
	95	(1.707, 2.575)	(1.878, 2.923)	(1.884, 2.935)			
	100	(0.985, 1.876)	(1.014, 1.974)				
	105	(0.597, 1.339)					
M	60	(4.435, 4.510)	(8.032, 8.239)	(10.875, 11.235)	(12.972, 13.522)	(14.356, 15.125)	(15.083, 16.013)
	65	(4.359, 4.477)	(7.792, 8.072)	(10.314, 10.840)	(11.989, 12.758)	(12.866, 13.841)	(13.185, 14.250)
	70	(4.231, 4.419)	(7.330, 7.822)	(9.397, 10.193)	(10.471, 11.529)	(10.841, 12.021)	(10.907, 12.108)
	75	(4.029, 4.307)	(6.689, 7.336)	(8.064, 9.028)	(8.527, 9.679)	(8.615, 9.792)	(8.619, 9.799)
	80	(3.653, 4.073)	(5.524, 6.387)	(6.143, 7.247)	(6.251, 7.420)	(6.256, 7.428)	(6.256, 7.428)
	85	(3.050, 3.626)	(4.017, 4.996)	(4.182, 5.267)	(4.193, 5.295)	(4.193, 5.296)	
	90	(2.121, 2.916)	(2.460, 3.512)	(2.484, 3.556)	(2.485, 3.558)		
	95	(1.383, 2.171)	(1.467, 2.361)	(1.468, 2.367)			
	100	(0.769, 1.611)	(0.788, 1.665)				
	105	(0.508, 1.220)					
<u>Weighted CoDa</u>							
F	60	(4.439, 4.521)	(8.048, 8.268)	(10.904, 11.318)	(13.100, 13.715)	(14.752, 15.548)	(15.881, 16.836)
	65	(4.366, 4.488)	(7.813, 8.130)	(10.476, 11.016)	(12.469, 13.234)	(13.829, 14.795)	(14.517, 15.672)
	70	(4.252, 4.444)	(7.498, 7.982)	(9.980, 10.708)	(11.632, 12.622)	(12.502, 13.719)	(12.751, 14.078)
	75	(4.198, 4.404)	(7.323, 7.829)	(9.422, 10.264)	(10.507, 11.658)	(10.836, 12.116)	(10.877, 12.180)
	80	(4.028, 4.353)	(6.725, 7.514)	(8.103, 9.312)	(8.512, 9.937)	(8.573, 10.024)	(8.575, 10.031)
	85	(3.676, 4.189)	(5.541, 6.616)	(6.095, 7.418)	(6.166, 7.547)	(6.168, 7.552)	
	90	(2.891, 3.607)	(3.746, 4.848)	(3.858, 5.048)	(3.865, 5.057)		
	95	(2.094, 2.757)	(2.355, 3.205)	(2.368, 3.228)			
	100	(1.321, 1.813)	(1.375, 1.907)				
	105	(0.821, 1.148)					

M	60	(4.423, 4.515)	(8.032, 8.267)	(10.936, 11.351)	(13.218, 13.833)	(14.859, 15.712)	(15.863, 16.939)
	65	(4.371, 4.496)	(7.883, 8.202)	(10.612, 11.177)	(12.611, 13.443)	(13.781, 14.930)	(14.273, 15.607)
	70	(4.300, 4.488)	(7.651, 8.128)	(10.030, 10.908)	(11.500, 12.751)	(12.061, 13.543)	(12.187, 13.713)
	75	(4.146, 4.443)	(7.102, 7.877)	(8.908, 10.119)	(9.649, 11.116)	(9.767, 11.342)	(9.777, 11.361)
	80	(3.841, 4.330)	(6.119, 7.239)	(6.996, 8.562)	(7.192, 8.846)	(7.207, 8.872)	(7.207, 8.873)
	85	(3.231, 3.936)	(4.483, 5.749)	(4.736, 6.159)	(4.756, 6.191)	(4.757, 6.192)	
	90	(2.411, 3.123)	(2.891, 3.846)	(2.926, 3.900)	(2.927, 3.900)		
	95	(1.640, 2.125)	(1.747, 2.291)	(1.749, 2.296)			
	100	(0.953, 1.303)	(0.975, 1.336)				
	105	(0.582, 0.896)					

Appendix A presents the point estimate of annuity prices for various ages and maturities when the interest rate $\zeta = 1\%$ and 5% , respectively. In Appendix B, we show the 95% pointwise prediction intervals.

8 Conclusion

We present an extension of the CoDa method by incorporating geometrically decaying weights to estimate mean function and functional principal components. The weighted CoDa method can improve the forecast accuracy of age-specific life-table death counts, which could help actuaries enhance the accuracy of their pricing of annuities and setting of reserves.

In the weighted CoDa method, larger weights are assigned to the most recent data, whereas the data from the distant past are less important to forecasting. We select the estimated optimal value of the weight parameter by minimizing the KLD and two variants of the JSD using a set of validation data. We compare the point forecast errors between the standard and weighted CoDa methods in the testing data with the estimated weight parameter. The weighted CoDa method generally improves accuracy compared with its unweighted counterparts.

From the viewpoint of forecast accuracy, we suggest implementing the weighted CoDa method. From the perspective of actuarial calculations, the improvement in mortality leads to a more accurate estimate of annuity prices. To facilitate reproducibility, the  code for implementing all the methods is available at https://github.com/hanshang/Weighted_CoDa.

There are a few ways in which the present paper can be further extended, and we briefly mention five: 1) Although we demonstrate the practicability of the proposal via the Swedish data, the weighted CoDa method can be applied to other countries (such as Denmark, Japan, and the USA), especially with long-run high-quality mortality data. 2) One could implement a hypothesis test, such as the Friedman and Nemenyi tests in [Shang \(2015\)](#), to examine the statistical significance between the standard and weighted CoDa methods. 3) One could study the uncertainty associated with the estimated weight parameter. 4) One could apply the weighted CoDa method to death counts from cohort-based life tables. 5) Centered log-ratio transformation

is one of many possible transformations. We may also study additive log-ratio transformation in [Aitchison \(1986\)](#), square-root transformation in [Scealy & Welsh \(2011\)](#) or α transformation in [Tsagris & Stewart \(2020\)](#).

Acknowledgment

The authors thank a reviewer for insightful comments and suggestions. The first author acknowledges financial support from an Australian Research Council Discovery Project DP230102250.

Appendix A Estimate of annuity prices when interest rate $\zeta = 1\%$ or 5%

In Tables 7, we present the estimated annuity premium prices with \$1 benefit for various ages and maturities when the interest rate $\zeta = 1\%$.

Table 7 Estimates of annuity prices with various ages and maturities (T) for female and male policyholders residing in Sweden, when the interest rate is set at 1%.

Age	CoDa						Weighted CoDa					
	$T = 5$	10	15	20	25	30	5	10	15	20	25	30
Female												
60	4.791	9.213	13.224	16.743	19.615	21.582	4.789	9.198	13.184	16.663	19.485	21.426
65	4.756	9.071	12.856	15.945	18.061	19.078	4.748	9.040	12.786	15.824	17.914	18.931
70	4.701	8.825	12.191	14.496	15.604	15.896	4.690	8.784	12.104	14.388	15.499	15.802
75	4.594	8.344	10.912	12.146	12.472	12.508	4.578	8.291	10.845	12.088	12.425	12.465
80	4.360	7.346	8.781	9.160	9.202	9.204	4.345	7.335	8.790	9.185	9.231	9.233
85	3.853	5.705	6.194	6.248	6.250		3.874	5.760	6.272	6.332	6.335	
90	3.047	3.853	3.942	3.945			3.076	3.912	4.010	4.014		
95	2.132	2.367	2.377				2.178	2.432	2.443			
100	1.377	1.430					1.415	1.475				
105	0.906						0.940					
Male												
60	4.757	9.065	12.848	15.989	18.299	19.620	4.758	9.072	12.866	16.023	18.355	19.698
65	4.695	8.818	12.241	14.758	16.199	16.718	4.699	8.833	12.272	14.812	16.275	16.806
70	4.600	8.419	11.227	12.835	13.414	13.516	4.606	8.438	11.268	12.898	13.489	13.595
75	4.424	7.678	9.540	10.211	10.329	10.338	4.430	7.702	9.586	10.269	10.391	10.400
80	4.061	6.384	7.221	7.369	7.380	7.380	4.074	6.421	7.272	7.424	7.435	7.436
85	3.427	4.662	4.880	4.896	4.896		3.439	4.686	4.909	4.925	4.925	
90	2.560	3.013	3.046	3.046			2.571	3.031	3.064	3.065		
95	1.745	1.870	1.873				1.754	1.880	1.883			
100	1.152	1.183					1.155	1.186				
105	0.804						0.807					

In Tables 8, we present the estimated annuity premium prices with \$1 benefit for various ages and maturities when the interest rate $\zeta = 5\%$.

Table 8 Estimates of annuity prices with various ages and maturities (T) for female and male policyholders residing in Sweden, when the interest rate is set at 5%.

Age	CoDa						Weighted CoDa					
	$T = 5$	10	15	20	25	30	5	10	15	20	25	30
Female												
60	4.261	7.482	9.874	11.594	12.745	13.394	4.259	7.471	9.849	11.549	12.681	13.320
65	4.231	7.375	9.634	11.147	11.998	12.336	4.224	7.351	9.588	11.075	11.916	12.254
70	4.183	7.190	9.203	10.336	10.786	10.884	4.174	7.159	9.145	10.268	10.718	10.819
75	4.091	6.830	8.372	8.983	9.117	9.129	4.077	6.789	8.323	8.938	9.076	9.090
80	3.889	6.080	6.947	7.138	7.155	7.155	3.877	6.069	6.949	7.147	7.166	7.167
85	3.452	4.819	5.119	5.146	5.147		3.470	4.863	5.176	5.206	5.207	
90	2.750	3.352	3.407	3.409			2.775	3.399	3.460	3.462		
95	1.946	2.124	2.130				1.986	2.179	2.186			
100	1.272	1.313					1.306	1.353				
105	0.846						0.876					
Male												
60	4.232	7.370	9.629	11.165	12.094	12.531	4.233	7.376	9.640	11.185	12.122	12.566
65	4.178	7.184	9.230	10.465	11.047	11.220	4.182	7.195	9.251	10.497	11.088	11.265
70	4.096	6.884	8.567	9.360	9.596	9.631	4.101	6.899	8.595	9.399	9.640	9.676
75	3.944	6.327	7.449	7.783	7.832	7.835	3.950	6.344	7.480	7.820	7.870	7.873
80	3.631	5.341	5.850	5.925	5.929	5.929	3.643	5.370	5.888	5.964	5.969	5.969
85	3.081	3.999	4.133	4.141	4.141		3.092	4.018	4.155	4.163	4.163	
90	2.324	2.664	2.684	2.684			2.333	2.678	2.699	2.699		
95	1.602	1.697	1.699				1.610	1.706	1.708			
100	1.070	1.093					1.072	1.096				
105	0.752						0.755					

Appendix B Ninety-five percentage prediction intervals of annuity prices when interest rate $\zeta = 1\%$ or 5%

Table 9 Ninety-five percentage pointwise prediction intervals of annuity prices with different ages and maturities (T), when the interest rate $\zeta = 1\%$.

Sex	Age	$T = 5$	$T = 10$	$T = 15$	$T = 20$	$T = 25$	$T = 30$
<u>CoDa</u>							
F	60	(4.760, 4.809)	(9.117, 9.270)	(13.043, 13.355)	(16.497, 16.990)	(19.302, 20.034)	(21.240, 22.255)
	65	(4.702, 4.789)	(8.946, 9.172)	(12.645, 13.075)	(15.662, 16.349)	(17.739, 18.760)	(18.735, 20.052)
	70	(4.619, 4.760)	(8.647, 9.011)	(11.923, 12.584)	(14.180, 15.189)	(15.251, 16.593)	(15.550, 17.013)
	75	(4.502, 4.694)	(8.144, 8.665)	(10.668, 11.564)	(11.871, 13.124)	(12.190, 13.577)	(12.248, 13.648)
	80	(4.226, 4.543)	(7.102, 7.911)	(8.460, 9.721)	(8.800, 10.257)	(8.842, 10.349)	(8.844, 10.352)
	85	(3.670, 4.179)	(5.371, 6.504)	(5.813, 7.224)	(5.857, 7.335)	(5.859, 7.341)	
	90	(2.759, 3.582)	(3.424, 4.719)	(3.508, 4.866)	(3.510, 4.880)		
	95	(1.779, 2.702)	(1.989, 3.106)	(1.995, 3.135)			
	100	(1.020, 1.960)	(1.054, 2.077)				
	105	(0.615, 1.390)					
M	60	(4.703, 4.784)	(8.917, 9.156)	(12.600, 13.036)	(15.592, 16.314)	(17.762, 18.842)	(19.019, 20.410)
	65	(4.622, 4.748)	(8.642, 8.964)	(11.901, 12.549)	(14.288, 15.295)	(15.662, 17.007)	(16.202, 17.703)
	70	(4.484, 4.685)	(8.108, 8.673)	(10.775, 11.744)	(12.296, 13.657)	(12.901, 14.435)	(13.006, 14.583)
	75	(4.268, 4.565)	(7.374, 8.110)	(9.141, 10.297)	(9.786, 11.221)	(9.934, 11.404)	(9.942, 11.419)
	80	(3.864, 4.310)	(6.043, 7.010)	(6.851, 8.127)	(6.988, 8.382)	(7.005, 8.392)	(7.006, 8.393)
	85	(3.212, 3.831)	(4.333, 5.434)	(4.557, 5.778)	(4.574, 5.810)	(4.575, 5.811)	
	90	(2.226, 3.070)	(2.621, 3.766)	(2.651, 3.821)	(2.652, 3.824)		
	95	(1.443, 2.271)	(1.531, 2.493)	(1.533, 2.500)			
	100	(0.800, 1.675)	(0.818, 1.748)				
	105	(0.526, 1.266)					
<u>Weighted CoDa</u>							
F	60	(4.707, 4.796)	(8.933, 9.188)	(12.634, 13.139)	(15.768, 16.565)	(18.379, 19.471)	(20.358, 21.736)
	65	(4.629, 4.760)	(8.666, 9.028)	(12.108, 12.771)	(14.958, 15.943)	(17.102, 18.414)	(18.279, 19.953)
	70	(4.505, 4.712)	(8.309, 8.859)	(11.509, 12.384)	(13.868, 15.142)	(15.247, 16.873)	(15.680, 17.491)
	75	(4.448, 4.670)	(8.108, 8.682)	(10.810, 11.841)	(12.348, 13.840)	(12.812, 14.548)	(12.878, 14.662)
	80	(4.264, 4.614)	(7.414, 8.319)	(9.189, 10.639)	(9.763, 11.526)	(9.857, 11.672)	(9.861, 11.681)
	85	(3.888, 4.438)	(6.055, 7.275)	(6.759, 8.301)	(6.855, 8.469)	(6.860, 8.478)	
	90	(3.048, 3.807)	(4.032, 5.254)	(4.185, 5.506)	(4.195, 5.521)		
	95	(2.195, 2.895)	(2.496, 3.417)	(2.510, 3.443)			
	100	(1.375, 1.888)	(1.439, 1.995)				
	105	(0.849, 1.190)					
M	60	(4.691, 4.789)	(8.921, 9.187)	(12.681, 13.186)	(15.937, 16.740)	(18.526, 19.720)	(20.259, 21.869)
	65	(4.635, 4.769)	(8.747, 9.113)	(12.281, 12.964)	(15.121, 16.225)	(16.966, 18.577)	(17.788, 19.747)
	70	(4.560, 4.760)	(8.478, 9.028)	(11.568, 12.631)	(13.621, 15.263)	(14.541, 16.518)	(14.746, 16.825)
	75	(4.396, 4.712)	(7.856, 8.733)	(10.180, 11.643)	(11.176, 13.079)	(11.373, 13.452)	(11.388, 13.466)
	80	(4.063, 4.589)	(6.715, 7.992)	(7.861, 9.695)	(8.124, 10.106)	(8.145, 10.135)	(8.145, 10.136)
	85	(3.410, 4.165)	(4.870, 6.267)	(5.188, 6.802)	(5.217, 6.849)	(5.218, 6.850)	
	90	(2.533, 3.287)	(3.089, 4.128)	(3.133, 4.193)	(3.134, 4.195)		
	95	(1.713, 2.226)	(1.835, 2.414)	(1.838, 2.419)			
	100	(0.988, 1.354)	(1.012, 1.391)				
	105	(0.601, 0.926)					

In Tables 9 and 10, we present the pointwise prediction intervals of annuity prices with different ages and maturities (T) for female and male policyholders residing in Sweden when the interest rate $\zeta = 1\%$ and 5% , respectively.

Table 10 Ninety-five percentage pointwise prediction intervals of annuity prices with different ages and maturities (T) when the interest rate $\zeta = 5\%$.

Sex	Age	$T = 5$	$T = 10$	$T = 15$	$T = 20$	$T = 25$	$T = 30$
<u>CoDa</u>							
F	60	(4.234, 4.277)	(7.410, 7.525)	(9.749, 9.961)	(11.443, 11.733)	(12.574, 12.946)	(13.222, 13.677)
	65	(4.183, 4.259)	(7.278, 7.452)	(9.488, 9.779)	(10.979, 11.378)	(11.808, 12.343)	(12.145, 12.757)
	70	(4.109, 4.234)	(7.048, 7.331)	(9.020, 9.466)	(10.130, 10.732)	(10.570, 11.303)	(10.678, 11.442)
	75	(4.010, 4.178)	(6.672, 7.073)	(8.208, 8.805)	(8.797, 9.581)	(8.936, 9.757)	(8.951, 9.778)
	80	(3.773, 4.050)	(5.890, 6.512)	(6.713, 7.603)	(6.879, 7.874)	(6.900, 7.899)	(6.900, 7.899)
	85	(3.294, 3.735)	(4.542, 5.438)	(4.818, 5.882)	(4.845, 5.928)	(4.845, 5.930)	
	90	(2.490, 3.228)	(3.004, 4.066)	(3.054, 4.148)	(3.056, 4.154)		
	95	(1.636, 2.456)	(1.783, 2.757)	(1.788, 2.765)			
	100	(0.950, 1.796)	(0.976, 1.880)				
	105	(0.579, 1.292)					
M	60	(4.185, 4.255)	(7.258, 7.438)	(9.454, 9.753)	(10.932, 11.352)	(11.819, 12.365)	(12.224, 12.870)
	65	(4.115, 4.224)	(7.047, 7.293)	(9.004, 9.435)	(10.180, 10.771)	(10.740, 11.457)	(10.920, 11.686)
	70	(3.995, 4.170)	(6.653, 7.078)	(8.246, 8.908)	(9.002, 9.844)	(9.245, 10.158)	(9.279, 10.215)
	75	(3.806, 4.067)	(6.086, 6.657)	(7.161, 7.970)	(7.490, 8.419)	(7.549, 8.494)	(7.553, 8.499)
	80	(3.457, 3.850)	(5.067, 5.837)	(5.554, 6.504)	(5.623, 6.616)	(5.628, 6.621)	(5.628, 6.621)
	85	(2.895, 3.436)	(3.728, 4.610)	(3.856, 4.819)	(3.863, 4.839)	(3.864, 4.840)	
	90	(2.024, 2.774)	(2.318, 3.290)	(2.333, 3.321)	(2.333, 3.325)		
	95	(1.325, 2.077)	(1.402, 2.242)	(1.406, 2.248)			
	100	(0.740, 1.546)	(0.761, 1.598)				
	105	(0.491, 1.177)					
<u>Weighted CoDa</u>							
F	60	(4.189, 4.266)	(7.272, 7.465)	(9.481, 9.822)	(11.019, 11.495)	(12.067, 12.654)	(12.712, 13.389)
	65	(4.122, 4.234)	(7.068, 7.344)	(9.130, 9.571)	(10.526, 11.125)	(11.388, 12.108)	(11.801, 12.613)
	70	(4.015, 4.194)	(6.790, 7.216)	(8.710, 9.320)	(9.861, 10.654)	(10.429, 11.347)	(10.589, 11.560)
	75	(3.965, 4.157)	(6.635, 7.083)	(8.269, 8.968)	(9.041, 9.945)	(9.244, 10.222)	(9.277, 10.264)
	80	(3.805, 4.110)	(6.118, 6.809)	(7.202, 8.207)	(7.491, 8.631)	(7.528, 8.695)	(7.530, 8.698)
	85	(3.478, 3.958)	(5.078, 6.034)	(5.526, 6.666)	(5.576, 6.749)	(5.578, 6.752)	
	90	(2.749, 3.416)	(3.487, 4.488)	(3.581, 4.643)	(3.583, 4.649)		
	95	(1.998, 2.626)	(2.223, 3.015)	(2.232, 3.033)			
	100	(1.268, 1.740)	(1.318, 1.821)				
	105	(0.793, 1.108)					
M	60	(4.174, 4.260)	(7.256, 7.463)	(9.504, 9.844)	(11.099, 11.579)	(12.144, 12.764)	(12.712, 13.468)
	65	(4.126, 4.243)	(7.124, 7.406)	(9.240, 9.703)	(10.641, 11.287)	(11.396, 12.227)	(11.681, 12.612)
	70	(4.059, 4.235)	(6.922, 7.342)	(8.773, 9.491)	(9.784, 10.777)	(10.170, 11.288)	(10.232, 11.374)
	75	(3.913, 4.193)	(6.447, 7.128)	(7.848, 8.856)	(8.383, 9.551)	(8.477, 9.690)	(8.484, 9.702)
	80	(3.633, 4.089)	(5.595, 6.577)	(6.279, 7.599)	(6.401, 7.807)	(6.408, 7.818)	(6.409, 7.819)
	85	(3.061, 3.723)	(4.138, 5.280)	(4.333, 5.591)	(4.345, 5.617)	(4.345, 5.617)	
	90	(2.295, 2.965)	(2.715, 3.590)	(2.743, 3.632)	(2.744, 3.632)		
	95	(1.574, 2.033)	(1.664, 2.177)	(1.667, 2.181)			
	100	(0.920, 1.254)	(0.939, 1.281)				
	105	(0.563, 0.867)					

References

Aburto, J. M. & van Raalte, A. A. (2018), 'Lifespan dispersion in times of life expectancy fluctuation: The case of central and eastern Europe', *Demography* **55**, 2071–2096.

Aburto, J. M., Villavicencio, F., Basellini, U., Kjaergaard, S. & Vaupel, J. W. (2020), 'Dynamics of life expectancy and life span equality', *Proceedings of the National Academy of Sciences of the United States of America* **117**(10), 5250–5259.

Aitchison, J. (1982), 'The statistical analysis of compositional data', *Journal of the Royal Statistical Society: Series B* **44**(2), 139–177.

Aitchison, J. (1986), *The Statistical Analysis of Compositional Data*, Chapman & Hall, London.

Aitchison, J. & Shen, S. M. (1980), 'Logistic-normal distributions: Some properties and uses', *Biometrika* **67**(2), 261–272.

Barceló, C., Pawlowsky, V. & Grunsky, E. (1996), 'Some aspects of transformations of compositional data and the identification of outliers', *Mathematical Geology* **28**, 501–518.

Basellini, U., Kjaergaard, S. & Camarda, C. G. (2020), 'An age-at-death distribution approach to forecast cohort mortality', *Insurance: Mathematics & Economics* **91**, 129–143.

Bergeron-Boucher, M.-P., Canudas-Romo, V., Oeppen, J. & Vaupel, J. W. (2017), 'Coherent forecasts of mortality with compositional data analysis', *Demographic Research* **37**, 527–566.

Bergeron-Boucher, M.-P., Simonacci, V., Oeppen, J. & Gallo, M. (2018), 'Coherent modeling and forecasting of mortality patterns for subpopulations using multiway analysis of compositions: An application to Canadian provinces and territories', *The North American Actuarial Journal* **22**(1), 92–118.

Booth, H. (2006), 'Demographic forecasting: 1980 to 2005 in review', *International Journal of Forecasting* **22**(3), 547–581.

Booth, H. & Tickle, L. (2008), 'Mortality modelling and forecasting: A review of methods', *Annals of Actuarial Science* **3**(1-2), 3–43.

Brouhns, N., Denuit, M. & Vermunt, J. K. (2002), 'A poisson log-bilinear regression approach to the construction of projected lifetables', *Insurance: Mathematics and Economics* **31**(3), 373–393.

Cannon, E. & Tonks, I. (2008), *Annuity Markets*, Oxford University Press, Oxford.

Canudas-Romo, V. (2010), 'Three measures of longevity: Time trends and record values', *Demography* **47**(2), 299–312.

Cheung, S. L. K., Robine, J.-M., Tu, E. J.-C. & Caselli, G. (2005), 'Three dimensions of the survival curve: Horizontalization, verticalization, and longevity extension', *Demography* **42**(2), 243–258.

Debón, A., Chaves, L., Haberman, S. & Villa, F. (2017), 'Characterization of between-group inequality of longevity in EU countries', *Insurance: Mathematics and Economics* **75**, 151–165.

Delicado, P. (2011), 'Dimensionality reduction when data are density functions', *Computational Statistics and Data Analysis* **55**(1), 401–420.

Denuit, M., Devolder, P. & Goderniaux, A.-C. (2007), 'Securitization of longevity risk: Pricing survivor bonds with Wang transform in the Lee-Carter framework', *The Journal of Risk and Insurance* **74**(1), 87–113.

Dickson, D. C. M., Hardy, M. R. & Waters, H. R. (2009), *Actuarial Mathematics for Life Contingent Risks*, Cambridge University Press, Cambridge.

Fry, J. M., Fry, T. R. L. & McLaren, K. R. (1996), 'The stochastic specification of demand share equations: Restricting budget shares to the unit simplex', *Journal of Econometrics* **73**, 377–385.

Fuglede, B. & Topsøe, F. (2004), Jensen-Shannon divergence and Hilbert space embedding, in 'Proceedings of International Symposium on Information Theory'.

Glei, D., Lundström, H. & Wilmoth, J. (2007), About mortality data for Sweden, Working paper, Human Mortality Database.

URL: <https://www.mortality.org/File/GetDocument/hmd.v6/SWE/Public/InputDB/SWEcom.pdf>

Horiuchi, S., Ouellette, N., Cheung, S. L. K. & Robine, J.-M. (2013), 'Modal age at death: Lifespan indicator in the era of longevity extension', *Vienna Yearbook of Population Research* **11**, 37–69.

Human Mortality Database (2024), *University of California, Berkeley (USA), and Max Planck Institute for Demographic Research (Germany)*. Accessed on August 26, 2023.

URL: <http://www.mortality.org>

Hyndman, R. (2023), *demography: Forecasting Mortality, Fertility, Migration and Population Data*. R package version 2.0.

URL: <https://CRAN.R-project.org/package=demography>

Hyndman, R. J., Booth, H. & Yasmeen, F. (2013), 'Coherent mortality forecasting: the product-ratio method with functional time series models', *Demography* **50**(1), 261–283.

Hyndman, R. J. & Shang, H. L. (2009), 'Forecasting functional time series (with discussions)', *Journal of the Korean Statistical Society* **38**(3), 199–221.

Kokoszka, P., Miao, H., Petersen, A. & Shang, H. L. (2019), 'Forecasting of density functions with an application to cross-sectional and intraday returns', *International Journal of Forecasting* **35**(4), 1304–1317.

Kullback, S. & Leibler, R. A. (1951), 'On information and sufficiency', *Annals of Mathematical Statistics* **22**(1), 79–86.

Larsson, D. (2020), 'Diseases in early modern Sweden', *Scandinavian Journal of History* **45**(4), 407–432.

Lee, R. D. & Carter, L. R. (1992), 'Modeling and forecasting U.S. mortality', *Journal of the American Statistical Association: Applications & Case Studies* **87**(419), 659–671.

Li, D., Robinson, P. M. & Shang, H. L. (2020), 'Long-range dependent curve time series', *Journal of the American Statistical Association: Theory and Methods* **115**(530), 957–971.

Oeppen, J. (2008), Coherent forecasting of multiple-decrement life tables: A test using Japanese cause of death data, in 'European Population Conference', Barcelona, Spain.

URL: <http://epc2008.princeton.edu/papers/80611>

Paparoditis, E. (2018), 'Sieve bootstrap for functional time series', *The Annals of Statistics* **46**(6B), 3510–3538.

Paparoditis, E. & Shang, H. L. (2023), 'Bootstrap prediction bands for functional time series', *Journal of the American Statistical Association: Theory and Methods* **118**(542), 972–986.

Pawlowsky-Glahn, V., Egozcue, J. & Tolosana-Delgado, R. (2015), *Modeling and Analysis of Compositional Data*, John Wiley & Sons, Ltd, Chichester.

Preston, S., Heuveline, P. & Guillot, M. (2001), *Demography: Measuring and Modeling Population Processes*, Blackwell Publishers, Oxford, U.K.

Renshaw, A. E. & Haberman, S. (2003), 'Lee-Carter mortality forecasting with age-specific enhancement', *Insurance: Mathematics and Economics* **33**(2), 255–272.

Robine, J.-M. (2001), 'Redefining the stages of the epidemiological transition by a study of the dispersion of life spans: The case of France', *Population: An English Selection* **13**(1), 173–193.

Romano, E., Irpino, A. & Mateu, J. (2021), Spatial functional data analysis for probability density functions: compositional functional data vs. distributional data approach, in J. Mateu & R. Giraldo, eds, 'Geostatistical Functional Data Analysis', Wiley, Hoboken, New Jersey.

Scealy, J. L., de Caritat, P., Grunsky, E. C., Tsagris, M. T. & Welsh, A. H. (2017), 'Robust principal component analysis for power transformed compositional data', *Journal of the American Statistical Association: Theory and Methods* **110**(509), 136–148.

Scealy, J. L. & Welsh, A. H. (2011), 'Regression for compositional data by using distributions defined on the hypersphere', *Journal of the Royal Statistical Society: Series B* **73**(3), 351–375.

Scealy, J. L. & Welsh, A. H. (2017), 'A directional mixed effects model for compositional expenditure data', *Journal of the American Statistical Association: Applications and Case Studies* **112**(517), 24–36.

Shang, H. L. (2015), 'Statistically tested comparisons of the accuracy of forecasting methods for age-specific and sex-specific mortality and life expectancy', *Population Studies* **69**(3), 317–335.

Shang, H. L. (2018), 'Bootstrap methods for stationary functional time series', *Statistics and Computing* **28**(1), 1–10.

Shang, H. L. & Haberman, S. (2017), 'Grouped multivariate and functional time series forecasting: An application to annuity pricing', *Insurance: Mathematics and Economics* **75**, 166–179.

Shang, H. L. & Haberman, S. (2020), 'Forecasting age distribution of death counts: An application to annuity pricing', *Annals of Actuarial Science* **14**(1), 150–169.

Shang, H. L., Haberman, S. & Xu, R. (2022), 'Multi-population modelling and forecasting life-table death counts', *Insurance: Mathematics and Economics* **106**, 239–253.

Shannon, C. E. (1948), 'A mathematical theory of communication', *Bell Labs Technical Journal* **27**(3), 379–423.

Shkolnikov, V. M., Andreev, E. E. & Begun, A. Z. (2003), 'Gini coefficient as a life table function: computation from discrete data, decomposition of differences and empirical examples', *Demographic Research* **8**, 305–358.

Stefanucci, M. & Mazzuco, S. (2022), 'Analysing cause-specific mortality trends using compositional functional data analysis', *Journal of the Royal Statistical Society: Series A* **185**(1), 61–83.

Tsagris, M. & Stewart, C. (2020), 'A folded model for compositional data analysis', *Australian and New Zealand Journal of Statistics* **62**(2), 249–277.

van Raalte, A. A. & Caswell, H. (2013), 'Perturbation analysis of indices of lifespan variability', *Demography* **50**(5), 1615–1640.

van Raalte, A. A., Martikainen, P. & Myrskylä, M. (2014), 'Lifespan variation by occupational class: Compression or stagnation over time?', *Demography* **51**, 73–95.

Vaupel, J. W., Zhang, Z. & van Raalte, A. A. (2011), 'Life expectancy and disparity: An international comparison of life table data', *BMJ Open* **1**(1), e000128.

Wilmoth, J. R. & Horiuchi, S. (1999), 'Rectangularization revisited: Variability of age at death within human populations', *Demography* **36**(4), 475–495.

Yaari, M. E. (1965), 'Uncertain lifetime, life insurance, and the theory of the consumer', *The Review of Economic Studies* **32**(2), 137–150.